final product. In contrast, no evidence for the formation of an analogous bis(diazenido) compound was detected by using different solvents and excess of arenediazonium salt. The different nature and/or properties of the diazene intermediate in iron and ruthenium complexes probably result in different final products in the reaction of η^2-H_2 derivatives with arenediazonium cations.

We also studied the reactivity of the dihydride precursor RuH_2P_4 toward arenediazonium cations in order to compare these results with those obtained with the dihydrogen complexes. We also wished to clarify the influence of the phosphite ligand on the reaction by comparison of our findings with our previous data[13b] on the hydride $RuH_2[P(OEt)_3]_4$. While the $RuH_2[P(OMe)_3]_4$ derivative reacts in CH_2Cl_2 or acetone with arenediazonium cations in a 1:1 ratio or in excess to give six-coordinate $[RuH(ArN{=}NH)P_4]^+$ (**8b**) and $[Ru(ArN{=}NH)_2P_4]^{2+}$ (**9b**) derivatives, respectively, the hydride $RuH_2[PhP(OEt)_2]_4$ reacts in both acetone or CH_2Cl_2 solution with an excess of ArN_2^+ to give a mixture of bis(diazene) $[Ru(ArN{=}NH)_2\{PhP(OEt)_2\}_4]^{2+}$ (**9a**) and the pentacoordinate $[Ru(ArN{=}NH)\{PhP(OEt)_2\}_4]^{2+}$ (**7a**) derivatives (ratio 5:1), from which the bis(diazene) can be separated in pure form by fractional crystallization. The same mixture was also obtained by reacting the $[RuH(ArN{=}NH)\{PhP(OEt)_2\}_4]^+$ compound with arenediazonium cations.

Since we observed that solutions of bis(aryldiazene) in acetone or dichloromethane slowly give the pentacoordinate $[Ru(ArN{=}NH)P_4]^{2+}$ complexes by dissociation of one of the diazene ligands, it is probable that the reaction between RuH_2P_4 and ArN_2^+ proceeds first to give the bis(diazene), which by slow dissociation affords the pentacoordinate $[Ru(ArN{=}NH)P_4]^{2+}$ derivatives found in the final reaction mixture. The dissociation of one diazene ligand from $[Ru(ArN{=}NH)_2\{PhP(OEt)_2\}_4]^{2+}$ complexes were observed, but not from the corresponding $P(OMe)_3$ and $P(OEt)_3$ compounds. This observation may reasonably be explained on the basis of the large steric hindrance of $PhP(OEt)_2$ as compared with the $P(OMe)_3$ and $P(OEt)_3$ ligands.

Some spectroscopic properties of both the mono- and bis(diazene) complexes are provided in Table I. These compounds have properties similar to those of the closely related $P(OEt)_3$ derivatives previously reported by us.[13b] The deprotonation reactions of both the $[Ru(ArN{=}NH)_2P_4]^{2+}$ and $[Ru(ArN{=}NH)P_4]^{2+}$ derivatives with NEt_3 proceed to give the pentacoordinate aryldiazenido $[Ru(ArN_2)P_4]BPh_4$ (**10**) complexes, which were isolated and characterized. The ν_{NN} at 1640 cm^{-1} (1624 cm^{-1} in the labeled ^{15}N compounds) in the IR spectra suggest for **10a** a singly bent ArN_2 group. The ABC_2 multiplets in the $^{31}P\{^1H\}$ NMR spectra like those in the spectra of the related iron derivatives[13a] indicate the existence in solution of a TBP geometry distorted toward SP. However, this result contrasts with those found for the $P(OEt)_3$ derivatives,[13b] in which the A_2B_2-type ^{31}P spectra suggest a regular TBP structure. Finally, it may be observed that the mono(aryldiazenido) complexes can easily be protonated by $HBF_4{\cdot}Et_2O$ to give the pentacoordinate $[Ru(ArN{=}NH)P_4](BPh_4)_2$ derivatives.

Acknowledgment. The financial support of MPI and CNR, Rome, is gratefully acknowledged. We thank Daniela Baldan for technical assitance.

Registry No. **1a**, 123752-69-2; **1a'**, 123752-68-1; **1a'$_1$**, 123753-16-2; **1*a**, 123752-74-9; **1*a'**, 123752-73-8; **1b'**, 123752-71-6; **1b'$_1$**, 123753-18-4; **1c'**, 123753-14-0; **1*c**, 123808-88-8; **1*c'**, 123752-76-1; **2a**, 86494-67-9; **3a**, 123752-78-3; **3*a'**, 123752-80-7; **3*c**, 123752-82-9; **4a**, 123752-84-1; **5a**, 123752-85-2; **6a**, 123752-87-4; **6*a**, 123752-89-6; **6*c**, 123752-91-0; **7a**, 123752-93-2; **7a'**, 123752-94-3; **7a$_1$**, 123752-96-5; **7a$_2$**, 123752-98-7; **7b**, 123753-00-4; **8a**, 123753-02-6; **8b**, 123753-04-8; **9a**, 123753-06-0; **9b**, 123753-08-2; **10a**, 123753-10-6; **10b**, 123753-12-8; $RuH_2[PhP(OEt)_2]_4$, 123877-52-1; $RuH_2[P(OMe)_3]_4$, 38784-31-5; $RuH_2[P(OEt)_3]_4$, 53495-34-4; $OsH_2[PhP(OEt)_2]_4$, 123753-19-5; $OsH_2[P(OEt)_3]_4$, 123753-20-8.

Supplementary Material Available: Melting point data and elemental analyses for the complexes (Table S1) (3 pages). Ordering information is given on any current masthead page.

Contribution from the Department of Inorganic Chemistry and Crystallography, University of Nijmegen, 6525 ED Nijmegen, The Netherlands

Electrophilic Addition Reactions of Ag^+ with $Pt(AuPPh_3)_8^{2+}$ and $Pt(CO)(AuPPh_3)_8^{2+}$. Crystal Structures of $[Pt(AgNO_3)(AuPPh_3)_8](NO_3)_2$ and $[Pt(CO)(AgNO_3)(AuPPh_3)_8](NO_3)_2$

R. P. F. Kanters, P. P. J. Schlebos, J. J. Bour, W. P. Bosman, J. M. M. Smits, P. T. Beurskens, and J. J. Steggerda*

Received March 15, 1989

$Pt(AuPPh_3)_8^{2+}$ (**1**) and $Pt(CO)(AuPPh_3)_8^{2+}$ (**2**) react with Ag^+, forming the addition products $PtAg(AuPPh_3)_8^{3+}$ (**3**) and $Pt(CO)Ag(AuPPh_3)_8^{3+}$ (**4**), respectively. Compound **3** is characterized by conductivity measurements, elemental analysis, IR and ^{31}P and ^{195}Pt NMR spectroscopy, and single-crystal X-ray diffraction of its nitrate (monoclinic, space group $P2/a$, a = 28.007 (18) Å, b = 17.748 (3) Å, c = 28.216 (4) Å, β = 99.12 (3)°, V = 13848 Å^3, Z = 4, residuals R = 0.048 and R_w = 0.071 for 3722 observed reflections and 495 variables, Mo Kα radiation). Compound **4** is characterized by elemental analysis, IR and ^{31}P, ^{13}C, and ^{195}Pt NMR spectroscopy, and single-crystal X-ray diffraction of its nitrate (triclinic, space group $P\bar{1}$, a = 17.4363 (24) Å, b = 20.358 (7) Å, c = 20.500 (3) Å, α = 94.18 (2)°, β = 93.20 (1)°, γ = 99.64 (2)°, V = 7138 Å^3, Z = 2, residuals R = 0.065 and R_w = 0.086 for 8383 observed reflections and 475 variables, Mo Kα radiation). In the metal clusters **3** and **4** the central Pt atom is surrounded by eight Au atoms and one Ag atom. The phosphines are attached to the Au atoms, and one nitrate is attached to the Ag atom. CO is μ_1-bonded to Pt in **4**. Both reactions show the electrophilic addition of a Ag^+ ion. The alternative synthesis of **4** by addition of CO to **3** shows the amphoteric behavior of the central Pt atom in this cluster compound.

Introduction

The addition of nucleophiles to centered gold or mixed platinum–gold clusters is well-known. In reactions 1 and 2 CO and

$$Pt(AuPPh_3)_8^{2+} + CO \rightarrow Pt(CO)(AuPPh_3)_8^{2+} \quad (1)$$

$$Au(AuPPh_3)_7^{2+} + PPh_3 \rightarrow Au(PPh_3)(AuPPh_3)_7^{2+} \quad (2)$$

PPh_3 are added to the central platinum and gold atoms, respectively.[1,2] These reactions can be described as Lewis base additions to the central metal atoms of the clusters. The electron configurations change, in both cases, from $(S^\sigma)^2(P^\sigma)^4$ to $(S^\sigma)^2(P^\sigma)^6$.[3,4]

(1) Kanters, R. P. F.; Schlebos, P. P. J.; Bour, J. J.; Bosman, W. P.; Behm, H. J.; Steggerda, J. J. *Inorg. Chem.* **1988**, *27*, 4034.
(2) van der Velden, J. W. A.; Bour, J. J.; Bosman, W. P.; Noordik, J. H. *Inorg. Chem.* **1983**, *22*, 1913.

0020-1669/90/1329-0324$02.50/0

The geometry around the central metal atom is changed from a toroidal to a spheroidal one. These reactions and geometry changes are analogous to those found in the chemistry of mononuclear transition-metal complexes, e.g. reaction 3.

$$Pt(PPh_3)_3 + CO \rightarrow Pt(PPh_3)_3(CO) \quad (3)$$

The electrophilic addition of Au(I) to centered Au clusters is demonstrated in reactions 4 and 5.[2,5] These reactions show the

$$Au(AuPPh_3)_7^{2+} + AuPPh_3^+ \rightarrow Au(AuPPh_3)_8^{3+} \quad (4)$$

$$Au(AuPMe_2Ph)_{10}^{3+} + 2AuCl(PMe_2Ph) \rightarrow Au(AuCl)_2(AuPMe_2Ph)_{10}^{3+} + 2PMe_2Ph \quad (5)$$

addition of an electron acceptor to an $(S^\sigma)^2(P^\sigma)^4$ and an $(S^\sigma)^2(P^\sigma)^6$ cluster, respectively. As the electron configurations does not change, the structure remains toroidal in reaction 4 and spheroidal in reaction 5.

The effects of the addition of an electron donor or acceptor on the bonding in gold clusters could be observed in changes of the structure. In Mössbauer spectra the different Au sites can be detected and an $(S^\sigma)^2(P^\sigma)^6$ configuration is apparent by the absence of a quadrupole pair for the central Au atom. In the case of mixed platinum–gold clusters, with the platinum atom in the center of the cluster, changes in bonding and electron distribution are also observable in ^{195}Pt and ^{31}P NMR data.

In this paper we report the electrophilic addition reactions of Ag^+ with the $Pt(AuPPh_3)_8^{2+}$ (**1**) and $Pt(CO)(AuPPh_3)_8^{2+}$ (**2**) clusters, as well as the nucleophilic addition of CO to $PtAg(AuPPh_3)_8^{3+}$ (**3**). It will be shown that Ag is incorporated in the Pt–Au frame with short Pt–Ag and Au–Ag bond lengths. Some complexes containing Pt and Ag have been structurally characterized.[6] Nearly all have bridging ligands between Pt and Ag. Unbridged Pt–Ag bonds are present in $[PtMe_2(bpy)(AgPPh_3)]^+$ and in $[\{PtMe_2(bpy)\}_2Ag]^+$.[7] An interesting Au–Ag cluster is known to have a $Au_{13}Ag_{12}$ frame.[8]

A preliminary report of this work has been published.[9]

Experimental Section

Measurements. Elemental analysis were carried out in the microanalytical department of the University of Nijmegen. ^{195}Pt NMR spectra of CD_2Cl_2 solutions were recorded on a Bruker WM-200 spectrometer operating at 43.0225 MHz with $PtCl_6^{2-}$ in D_2O as the external reference. $^{13}C\{^1H\}$ NMR spectra of CD_2Cl_2 solutions were recorded on the same apparatusa operating at 50.3234 MHz with a TMS reference. $^{31}P\{^1H\}$ NMR spectra of MeOH solutions were recorded on a VARIAN XL-100 FT instrument at 40.5 MHz with a TMP reference. Infrared spectra of CsI pellets were recorded on a Perkin-Elmer 283 instrument. Electrical conductivity measurements were performed with a Metrohm Konduktoskop and a Phillips PR 9510/00 conductivity cell.

Preparation of the Compounds. $[Pt(AuPPh_3)_8](NO_3)_2$ and $[Pt(CO)(AuPPh_3)_8](NO_3)_2$ were prepared by published methods.[1,10] The other reagents were obtained from commercial sources and used without further purification.

$[Pt(AgNO_3)(AuPPh_3)_8](NO_3)_2$ (3). A 50-mg (12.5-μmol) sample of $[Pt(AuPPh_3)_8](NO_3)_2$ is dissolved in 2 mL of methanol. Under vigorous stirring, 2.1 mg (12.5 μmol) of $AgNO_3$ in 1 mL of methanol is added dropwise. The color of the solution changes immediately from red-brown to dark brown. Dark brown crystals are obtained by slow diffusion of diethyl ether into the reaction mixture. The yield is nearly 100%.

Anal. Calcd for $PtAgAu_8P_8C_{144}H_{120}N_3O_9$ (mol. wt. 4163.06): Pt, 4.69; Ag, 2.59; Au, 37.85; P, 5.95; C, 41.55; H, 2.91; N, 1.01. Found: Pt, 4.45; Ag, 2.83; Au, 36.86; P, 5.50; C, 41.04; H, 3.10; N, 0.99. IR: $\nu(NO_3)$ 1355 (broad) and 1280 cm^{-1}; several PPh_3 absorption bands. ^{31}P NMR: δ = 57.0, with ^3J(P–Ag) (doublet) ≈ 19 Hz (broad lines). ^{195}Pt NMR: δ = −4376.2, with $^1J(Pt-^{109}Ag)$ (doublet) = 811 Hz, $^1J(Pt-^{107}Ag)$ (doublet) = 717 Hz, and $^2J(Pt-^{31}P)$ (nonet) = 453 Hz. Conductivity in acetone at 25 °C: Λ_0 = 399 $cm^2\ \Omega^{-1}\ mol^{-1}$.

$[Pt(CO)(AgNO_3)(AuPPh_3)_8](NO_3)_2$ (4). This compound can be prepared by two procedures:

A 50-mg (12.4-μmol) sample of $[Pt(CO)(AuPPh_3)_8](NO_3)_2$ is dissolved in 2 mL of methanol. Under vigorous stirring, 2.1 mg (12.5 μmol) of $AgNO_3$ in 1 mL of methanol is added dropwise. The color of the solution remains bright red.

A 50-mg (12.0-μmol) sample of $[Pt(AgNO_3)(AuPPh_3)_8](NO_3)_2$ is dissolved in 2 mL of methanol. CO gas is bubbled through the solution. The red-brown solution immediately turns to bright red.

Bright red crystals can be obtained by slow diffusion of diethyl ether into the methanol solutions; yields are nearly 100% for both methods.

The ^{13}CO product can be obtained in analogous ways by addition of Ag^+ to $Pt(^{13}CO)(AuPPh_3)_8^{2+}$ or by reacting $PtAg(AuPPh_3)_8^{3+}$ with ^{13}CO.

Anal. Calcd for $PtAgAu_8P_8C_{145}H_{120}N_3O_{10}$ (mol. wt. 4191.07): Pt, 4.65; Ag, 2.57; Au, 37.60; P, 5.91; C, 41.56; H, 2.89; N, 1.00. Found: Pt, 5.08; Ag, 2.70; Au, 36.21; P, 6.50; C, 40.96; H, 2.98; N, 1.00. IR: ν(CO) 1964 cm^{-1}; $\nu(^{13}CO)$ 1918 cm^{-1}; $\nu(NO_3)$ 1355 (broad) and 1290 cm^{-1}; several PPh_3 absorption bands. ^{13}C NMR: δ = 208.10, with $^1J(C-^{195}Pt)$ (doublet) = 1226 Hz, $^2J(C-^{107}Ag)$ (doublet) = 24 Hz, $^2J(C-^{109}Ag)$ (doublet) = 28 Hz, and $^3J(C-^{31}P)$ (nonet) = 10 Hz. ^{31}P NMR: δ = 54.7, with $^2J(P-^{195}Pt)$ (doublet) = 366 Hz and ^3J(P–Ag) (doublet) = 17 Hz. ^{195}Pt NMR: δ = −5688.0, with ^1J(Pt–Ag) (doublet) ≈ 370 Hz and $^2J(Pt-^{31}P)$ (nonet) ≈ 370 Hz (broad lines).

Structure Determination of $[Pt(AgNO_3)(AuPPh_3)_8](NO_3)_2$ (3) and $[Pt(CO)(AgNO_3)(AuPPh_3)_8](NO_3)_2$ (4). Collection and Reduction of Crystallographic Data. Since the single crystals decomposed very quickly upon removal from the solvent mixture, crystals of **3** and **4** were mounted in a capillary together with a mixture of methanol and diethyl ether. X-ray data were measured on an Enraf-Nonius CAD4 diffractometer at 293 K using monochromated Mo Kα radiation. The crystal data are listed in Table I. The data were collected by using the ω–2θ mode with a variable scan speed and a maximum scan time of 15 s/reflection. Three standard reflections were measured after every 1800 s of X-ray exposure time. After correction for Lorentz and polarization effects the equivalent reflections were averaged. No extinction correction was performed.

Solution and Refinement of the Structures. The positions of the metal atoms were found by the direct methods part of SHELXS.[11] The remaining non-hydrogen atoms were positioned from successive difference Fourier maps. The phenyl rings were treated as regular hexagons, and their hydrogen atoms were placed at ideal positions. The structures were refined by full-matrix least squares on F values by using SHELX.[12] Scattering factors were taken from ref 13. Isotropic refinement converged to residuals of 0.11 (**3**) and 0.12 (**4**). At this stage an empirical absorption correction was applied,[14] resulting in a further decrease of R

Table I. Crystal Data for $[Pt(AgNO_3)(AuPPh_3)_8](NO_3)_2$ and $[Pt(CO)(AgNO_3)(AuPPh_3)_8](NO_3)_2$

chem formula	$PtAgAu_8P_8C_{144}H_{120}N_3O_9$	$PtAgAu_8P_8C_{145}H_{120}N_3O_{10}$
fw	4163.02	4191.03
a, Å	28.007 (18)	17.4363 (24)
b, Å	17.748 (3)	20.358 (7)
c, Å	28.216 (4)	20.500 (3)
α, deg		94.18 (2)
β, deg	99.12 (3)	93.20 (1)
γ, deg		99.64 (2)
V, Å^3	13848	7138
Z	4	2
space group	$P2/a$ (No. 13)	$P\bar{1}$ (No. 1)
T, °C	20	20
λ, Å	0.713 59	0.713 59
ρ_{calc}, g cm^{-3}	1.997	1.950
μ(Mo Kα), cm^{-1}	97.14	94.24
$R(F_o)$	0.048	0.065
$R_w(F_o)$	0.071	0.086

(3) Stone, C. A. *Inorg. Chem.* **1981**, *20*, 563.
(4) Hall, K. P.; Mingos, D. M. P. In *Progress in Inorganic Chemistry*; Lippard, S. J., Ed.; John Wiley & Sons, Inc.: New York, 1984; Vol. 32, p 237.
(5) Briant, C. E.; Theobald, B. R. C.; White, J. W.; Bell, L. K.; Mingos, D. M. P.; Welch, A. J. *J. Chem. Soc., Chem. Commun.* **1981**, 201.
(6) Usón, R.; Forniés, J.; Tomás, M.; Casa, J. M.; Cotton, F. A.; Falvello, L. R. *Inorg. Chem.* **1986**, *25*, 4519 and references therein.
(7) Arsenault, G. J.; Anderson, C. M.; Puddephatt, R. J. *Organometallics* **1988**, *7*, 2094.
(8) Teo, B. K.; Keating, K. *J. Am. Chem. Soc.* **1984**, *106*, 2224.
(9) Kanters, R. P. F.; Bour, J. J.; Schlebos, P. P. J.; Steggerda, J. J. *J. Chem. Soc., Chem. Commun.* **1988**, 1634.
(10) Bour, J. J.; Kanters, R. P. F.; Schlebos, P. P. J.; Steggerda, J. J. *Recl. Trav. Chim. Pays-Bas* **1988**, *107*, 211.
(11) Sheldrick, G. M. *SHELXS-86, A Program for Crystal Structure Determination*; Institut für Anorganische Chemie der Universität Göttingen: Göttingen, FRG, 1986.
(12) Sheldrick, G. M. *SHELX, A Program for Crystal Structure Determination*; University Chemical Laboratory: Cambridge, UK, 1976.
(13) *International Tables for X-Ray Crystallography*; Kynoch: Birmingham, UK, 1978; Vol. IV.
(14) Walker, N.; Stuart, D. *Acta Crystallogr., Sect. A* **1983**, *A39*, 158.

Table II. Selected Fractional Positional and Thermal Parameters

atom	*x*	*y*	*z*	$100U_{eq}$[a]
		$[Pt(AgNO_3)(AuPPh_3)_8](NO_3)_2$		
Pt	0.024 45 (8)	0.225 95 (11)	0.263 36 (8)	2.51 (10)
Au1	0.051 31 (8)	0.349 25 (11)	0.221 04 (8)	3.19 (10)
Au2	0.043 15 (8)	0.083 19 (12)	0.287 71 (9)	3.61 (11)
Au3	0.057 44 (8)	0.204 94 (12)	0.354 07 (8)	3.15 (10)
Au4	−0.041 68 (8)	0.127 35 (12)	0.221 53 (8)	3.29 (10)
Au5	0.035 98 (8)	0.353 37 (12)	0.314 02 (8)	3.49 (11)
Au6	−0.052 32 (8)	0.295 60 (12)	0.217 66 (8)	3.46 (11)
Au7	0.115 47 (8)	0.270 65 (12)	0.294 57 (8)	3.29 (11)
Au8	0.011 93 (8)	0.222 51 (12)	0.169 82 (8)	3.34 (10)
Ag	−0.035 36 (15)	0.156 22 (24)	0.316 79 (15)	4.43 (20)
P1	0.084 2 (5)	0.452 1 (8)	0.190 2 (6)	4.3 (7)
P2	0.080 6 (5)	−0.031 9 (8)	0.299 5 (6)	4.3 (7)
P3	0.075 2 (5)	0.203 5 (8)	0.433 0 (5)	4.1 (7)
P4	−0.099 5 (5)	0.038 5 (8)	0.194 0 (5)	3.7 (7)
P5	0.005 8 (5)	0.453 6 (8)	0.348 3 (5)	4.3 (7)
P6	−0.126 8 (5)	0.350 2 (8)	0.196 6 (6)	4.1 (7)
P7	0.198 2 (5)	0.264 8 (8)	0.298 8 (6)	4.1 (7)
P8	0.024 9 (5)	0.188 3 (7)	0.097 4 (5)	3.5 (7)
O11	−0.106 0 (12)	0.162 2 (21)	0.345 1 (13)	6.3 (12)
		$[Pt(CO)(AgNO_3)(AuPPh_3)_8](NO_3)_2$		
Pt	0.183 15 (7)	0.246 02 (7)	0.715 03 (5)	3.58 (5)
Au1	0.299 43 (8)	0.178 03 (7)	0.743 63 (6)	5.16 (6)
Au2	0.049 05 (7)	0.291 15 (8)	0.686 51 (6)	5.30 (6)
Au3	0.126 91 (7)	0.319 88 (7)	0.815 82 (5)	4.02 (5)
Au4	0.171 09 (7)	0.300 48 (7)	0.594 36 (5)	4.50 (5)
Au5	0.290 63 (7)	0.309 38 (7)	0.809 16 (5)	4.41 (5)
Au6	0.321 03 (7)	0.300 68 (7)	0.672 41 (5)	4.23 (5)
Au7	0.169 37 (8)	0.192 27 (7)	0.832 87 (6)	5.31 (6)
Au8	0.232 13 (8)	0.177 66 (7)	0.609 43 (6)	5.29 (6)
Ag	0.202 28 (13)	0.383 19 (12)	0.712 24 (10)	4.12 (9)
P1	0.374 1 (6)	0.098 4 (6)	0.765 1 (5)	7.9 (5)
P2	−0.082 2 (5)	0.285 6 (5)	0.663 0 (4)	5.8 (4)
P3	0.076 4 (4)	0.386 6 (5)	0.893 4 (4)	4.6 (3)
P4	0.155 7 (5)	0.353 9 (5)	0.498 4 (4)	5.6 (4)
P5	0.376 3 (5)	0.374 3 (5)	0.888 0 (4)	5.6 (4)
P6	0.436 6 (5)	0.346 3 (5)	0.632 8 (4)	5.2 (4)
P7	0.114 8 (6)	0.123 2 (6)	0.907 8 (4)	6.9 (4)
P8	0.234 2 (6)	0.100 0 (5)	0.522 2 (5)	7.1 (4)
C1	0.108 5 (19)	0.168 5 (18)	0.693 9 (14)	5.4 (9)
O1	0.059 6 (16)	0.127 6 (15)	0.680 2 (12)	8.9 (8)
O11	0.257 7 (14)	0.493 5 (13)	0.707 0 (11)	7.7 (7)

[a] $U_{eq} = {}^1/_3\sum_i\sum_j a_i^* a_j^* a_i a_j U_{ij}$ in Å^2.

to 0.06 (**3**) and 0.09 (**4**). The positions of one nitrate (**3**) and of two nitrates (**4**) could be located. A large number of peaks in Fourier syntheses of **3** and **4**, found at positions between the cluster ions (at distances more than 3.5 Å from any atom), could not unambiguously be interpreted. They are ascribed to a mixture of (disordered) nitrate ions and solvent molecules. Some of these peaks suggested the geometry of nitrate or the solvent molecules, but none of them were found well enough to warrant inclusion in the refinement. During the final stage of the refinement, the anisotropic parameters of the gold, platinum, silver, and phosphorus atoms were refined. The phenyl groups were treated as rigid groups during the refinement. The hydrogen atoms were given fixed isotropic temperature factors of 0.06 Å^2. The function minimized was $\sum w(F_o - F_c)^2$ with $w = (\sigma^2(F_o) + 0.0008F_o^2)^{-1}$. Positional and thermal parameters of selected atoms are given in Table II, and selected bond distances and angles are provided in Table III. Structure factor tables and the positional parameters of the phenyl carbon and hydrogen atoms and of the residual peaks between the clusters are available as supplementary material.

Results

The transformations observed in this work are schematized in reaction 6.

$$\begin{array}{ccc} Pt(AuPPh_3)_8^{2+} & \xrightarrow{CO/acetone} & Pt(CO)(AuPPh_3)_8^{2+} \\ \mathbf{1} & & \mathbf{2} \\ {\scriptstyle Ag^+/MeOH}\downarrow & & \downarrow{\scriptstyle Ag^+/MeOH} \\ PtAg(AuPPh_3)_8^{3+} & \xrightarrow{CO/MeOH} & Pt(CO)Ag(AuPPh_3)_8^{3+} \\ \mathbf{3} & & \mathbf{4} \end{array} \qquad (6)$$

This shows the amphoteric character of the central atom in $Pt(AuPPh_3)_8^{2+}$ toward electron donors and acceptors.

Table III. Selected Bond Lengths (Å) and Bond Angles (deg) (with Esd's)

	$[Pt(AgNO_3)(AuPPh_3)_8](NO_3)_2$	$[Pt(CO)(AgNO_3)(AuPPh_3)_8](NO_3)_2$
Pt–Au1	2.658 (3)	2.7012 (21)
Pt–Au2	2.656 (3)	2.7017 (20)
Pt–Au3	2.607 (3)	2.7855 (18)
Pt–Au4	2.682 (3)	2.7952 (17)
Pt–Au5	2.668 (3)	2.7062 (16)
Pt–Au6	2.634 (3)	2.6949 (18)
Pt–Au7	2.684 (3)	2.7301 (18)
Pt–Au8	2.608 (3)	2.7419 (19)
Pt–Ag	2.722 (5)	2.7616 (30)
Au1–Au5	2.726 (3)	2.9352 (22)
Au1–Au6	3.042 (4)	2.9642 (22)
Au1–Au7	2.881 (3)	3.0299 (20)
Au1–Au8	2.804 (3)	2.9291 (18)
Au2–Au3	2.846 (3)	2.8842 (16)
Au2–Au4	2.888 (3)	2.9153 (18)
Au3–Au5	2.892 (3)	2.9083 (18)
Au3–Au7	2.772 (4)	2.8579 (23)
Au4–Au6	3.001 (3)	2.9874 (17)
Au4–Au8	2.816 (3)	2.9065 (23)
Au5–Au6	3.525 (3)	2.8804 (15)
Au5–Au7	2.793 (4)	2.9977 (20)
Au6–Au8	2.741 (4)	2.8891 (20)
Au2–Ag	2.786 (5)	2.9916 (26)
Au3–Ag	2.783 (5)	2.8356 (25)
Au4–Ag	2.714 (5)	2.8149 (24)
Au5–Ag	4.036 (5)	3.0738 (28)
Au6–Ag	3.708 (4)	2.9883 (29)
Au1–P1	2.280 (15)	2.295 (13)
Au2–P2	2.297 (14)	2.294 (9)
Au3–P3	2.204 (15)	2.332 (9)
Au4–P4	2.304 (14)	2.341 (9)
Au5–P5	2.252 (15)	2.312 (8)
Au6–P6	2.292 (14)	2.292 (8)
Au7–P7	2.303 (15)	2.296 (10)
Au8–P8	2.216 (15)	2.305 (10)
Pt–C1		1.877 (32)
Ag–O11	2.25 (4)	2.305 (26)
C1–O1		1.10 (4)
Au1–Pt–Au5	61.57 (9)	65.75 (6)
Au1–Pt–Au6	70.17 (11)	66.64 (6)
Au1–Pt–Au7	65.29 (10)	67.81 (6)
Au1–Pt–Au8	64.33 (9)	65.11 (5)
Au2–Pt–Au3	65.47 (5)	63.40 (5)
Au2–Pt–Au4	65.51 (10)	64.03 (5)
Au3–Pt–Au5	66.49 (9)	63.94 (5)
Au3–Pt–Au7	63.21 (10)	62.41 (5)
Au4–Pt–Au6	68.74 (10)	65.90 (5)
Au4–Pt–Au8	64.31 (10)	63.32 (5)
Au5–Pt–Au6	83.37 (11)	64.46 (5)
Au5–Pt–Au7	62.95 (11)	66.93 (5)
Au6–Pt–Au8	63.06 (10)	64.19 (5)
Au2–Pt–Ag	62.38 (13)	66.39 (8)
Au3–Pt–Ag	62.91 (13)	61.49 (7)
Au4–Pt–Ag	60.29 (12)	60.87 (6)
Au5–Pt–Ag	96.98 (13)	68.40 (7)
Au6–Pt–Ag	87.61 (15)	66.40 (7)
Pt–Au1–P1	172.5 (4)	166.10 (31)
Pt–Au2–P2	162.4 (4)	157.52 (27)
Pt–Au3–P3	169.1 (4)	175.35 (21)
Pt–Au4–P4	173.7 (4)	174.63 (24)
Pt–Au5–P5	151.4 (4)	173.47 (26)
Pt–Au6–P6	164.7 (4)	178.18 (21)
Pt–Au7–P7	154.1 (4)	156.89 (26)
Pt–Au8–P8	157.5 (4)	161.57 (27)
Pt–Ag–O11	145.9 (10)	162.2 (6)
Pt–C1–O1		172.6 (33)

The spectroscopic data obtained for the new compounds are given in Tables IV and V, discussed in the next section.

Discussion

Characterization and Crystal Structure of $[Pt(AgNO_3)(AuPPh_3)_8](NO_3)_2$ (3). In the solid the cluster ion has a central metal and nine peripheral metal atoms as shown in Figure 1.

Table IV. Coupling Constants

compd	coupling const, Hz					
	Pt–C	Pt–Ag	Pt–P	P–C	Ag–C	Ag–P
$Pt(AuPPh_3)_8^{2+}$			497			
$Pt(CO)(AuPPh_3)_8^{2+}$	1256		391	11		
$PtAg(AuPPh_3)_8^{3+}$		717	453			19
		811				
$Pt(CO)Ag(AuPPh_3)_8^{3+}$	1226	~370	366	10	24	17
					28	

Table V. Chemical Shifts

compd	chem shift, ppm		
	^{31}P	^{195}Pt	^{13}C
$Pt(AuPPh_3)_8^{2+}$	55.3	−4528.3	
$Pt(CO)(AuPPh_3)_8^{2+}$	51.3	−5456.7	210.7
$PtAg(AuPPh_3)_8^{3+}$	57.0	−4376.2	
$Pt(CO)Ag(AuPPh_3)_8^{3+}$	54.7	−5688.0	208.1

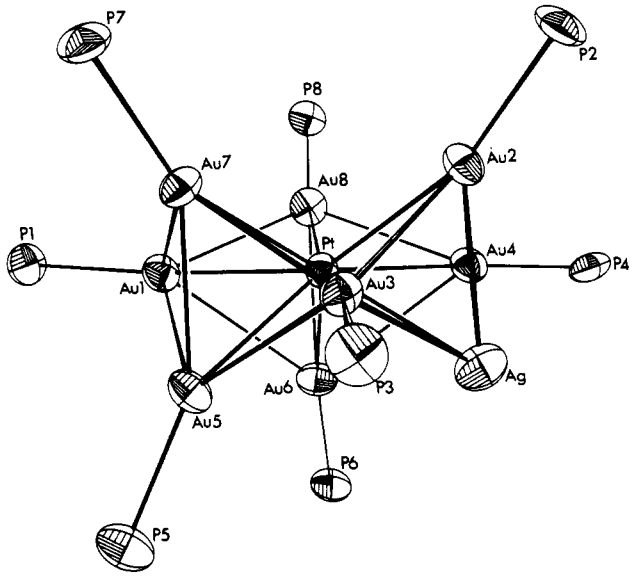

Figure 1. ORTEP drawing of the structure of **3**. Phenyl and nitrate groups are omitted for the sake of clarity.

Eight of these are bonded to phosphine. NMR data (vide infra) show that there is no direct Pt–P bond. We think that the central position is Pt and the periphery has eight Au atoms bonded to PPh_3 and one Ag atom bonded to nitrate. The central position of Pt in the parent compound **1**[10] as well as in **2**[1] and **4** could be firmly established by NMR considerations. The structure of the metal frame clearly shows the toroidal arrangement around the central metal atom, as could be expected from the electron count. The structure can be described as a torus formed by three staggered triangles, consisting of Au8–Au2–Au7, Au4–Au3–Au1, and Au6–Ag–Au5. The metal atoms in the top and bottom triangles are connected to four atoms, and those in the middle triangle to five other metal atoms, the Ag atom being in a triangle with the lowest connectivity. The structure is similar to that of the isoelectronic $[Au_{10}Cl_3(PCy_2Ph)_6](NO_3)$ cluster, which also has a connectivity of nine for the central metal atom.[15] The geometrical details are discussed after the description of structure **4**.

In the crystalline state one of the nitrate groups is very close to the Ag. No other nitrates were found within 3.5 Å of any metal atom; so we think that they are uncoordinated. This is also indicated by the IR spectrum where $\nu(NO_3)$ is found at 1280 and 1355 cm^{-1}, corresponding to coordinated and free nitrate, respectively. In an acetone solution the nitrate is dissociated from the Ag, as is shown by the large conductivity of the compound.

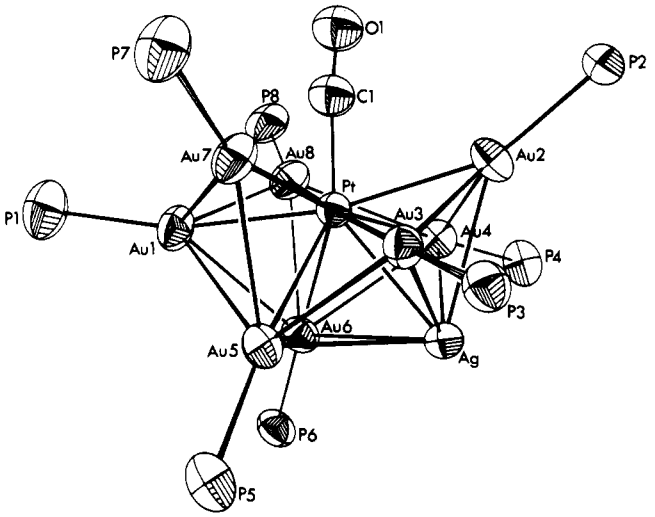

Figure 2. ORTEP drawing of the structure of **4**. Phenyl and nitrate groups and the CO oxygen atom are omitted for the sake of clarity.

The Λ_0 of 399 $cm^2\ \Omega^{-1}\ mol^{-1}$ indicates a 3:1 rather than a 2:1 electrolyte.

The ^{31}P NMR spectrum of **3** at room temperature consists of a singlet at $\delta = 57.0$ with a $^2J(^{31}P–^{195}Pt)$ of approximately 450 Hz with a line width of 50 Hz. At higher temperature (40 °C) $^3J(P–Ag)$ could be observed to be 19 Hz. Due to the line width (15 Hz) the separate ^{107}Ag and ^{109}Ag couplings could not be seen. This temperature dependency of the ^{31}P NMR spectra indicates that in addition to the fast fluxional behavior of phosphine sites, which is common in this type of cluster compounds,[16] another process with a relatively high coalescence temperature may be present. Another possibility is that Ag, which occupies a peripheral position, causes a larger difference in chemical shifts for different phosphine sites. This would result in an increase of the coalescence temperature for the exchange process. The nature of these rearrangements are still under investigation.

$^2J(^{31}P–^{195}Pt)$ decreases from 497 Hz in the parent compound to 453 Hz (see Table IV).[10] This must be related to the lowering of the Pt–Au bond order upon addition of Ag to the central metal atom, due to the fact that with the same number of bonding electrons an additional bond has to be maintained.

The ^{195}Pt NMR spectrum clearly shows the $Pt–^{107}Ag$ (717 Hz) and $Pt–^{109}Ag$ (811 Hz) through-bond coupling constants. Their ratio of 0.88 is in good agreement with the value of 0.87 expected from the gyromagnetic ratio. The chemical shift of −4376.2 ppm is shifted to higher frequency when compared with −4528.3 ppm found for the parent cluster **1** (see Table V). This indicates that Pt is less shielded after addition of Ag. This effect can also be seen in a more indirect way in the ^{31}P chemical shift, which shifts approximately 1.7 ppm to lower field.

Characterization and Crystal Structure of $[Pt(CO)(AgNO_3)(AuPPh_3)_8](NO_3)_2$ (4). The cluster has the same coordination geometry around the central atom as $Au(AuP(p\text{-}C_6H_4F)_3)_7(AuI)_3$,[17] both being $(S^\sigma)^2(P^\sigma)^6$ clusters with 10 coordinated central metal atoms; see Figure 2. When the structure of **4** is compared with that of **3**, the rearrangement from the toroidal to spheroidal geometry is clear. The two-electron-donating CO is bonded along the torus axis. This results in the formation of a P_z^σ bonding molecular orbital from the empty p_z^σ platinum orbital and the filled carbon σ orbital. The torus is also deformed by compressing the M_3 triangle opposite of CO toward the torus axis. The central metal atom is shifted into the hexagon formed by the two other triangles of $AuPPh_3$ groups.

The ^{31}P NMR spectrum of **4** consists of a singlet at $\delta = 54.7$ with ^{195}Pt satellites at 366 Hz. The singlet nature is a result of

(15) Briant, C. E.; Hall, K. P.; Wheeler, A. C.; Mingos, D. M. P. *J. Chem. Soc., Chem. Commun.* **1984**, 248.

(16) Vollenbroek, F. A.; van den Berg, J. P.; van der Velden, J. W. A.; Bour, J. J. *Inorg. Chem.* **1980**, *19*, 2685.

(17) Bellon, P.; Manassero, M.; Sansoni, M. *J. Chem. Soc., Dalton Trans.* **1972**, 1481.

Table VI. Selected Distances to the Pseudo Mirror Plane through the Atoms Pt, Au1, Au2, and Ag (in Å; Maximum Deviation 0.03 Å)

	$[Pt(AgNO_3)(AuPPh_3)_8](NO_3)_2$	$[Pt(CO)(AgNO_3)(AuPPh_3)_8](NO_3)_2$
Au3	−2.238 (3)	−2.320 (1)
Au4	+2.261 (3)	+2.327 (1)
Au5	−1.854 (3)	−1.508 (1)
Au6	+1.628 (3)	+1.370 (1)
Au7	−2.010 (3)	−2.346 (1)
Au8	+2.227 (3)	+2.410 (1)
C1		+0.22 (3)
O1		+0.34 (3)

the fluxional behavior in solution. The lowering of the chemical shift from 57.0 to 54.7 ppm on addition of CO to **3** can be attributed to the electronic differences between $(S^\sigma)^2(P^\sigma)^4$ and $(S^\sigma)^2(P^\sigma)^6$ cluster compounds.

The ^{13}C NMR spectrum shows that the chemical shift of ^{13}CO decreases on addition of Ag^+ to **2**. $^1J(^{13}C-^{195}Pt)$ decreases from 1256 to 1226 Hz. The two Ag isotopes give rise to different ^2J couplings, 24 and 28 Hz for ^{107}Ag and ^{109}Ag, respectively. These NMR data clearly indicate that CO is bonded to Pt, which is in the center of the metal frame.

The ^{195}Pt NMR spectrum consists of a multiplet, of an even number, of broad lines (~100 Hz) with separations of approximately 370 Hz. From ^{31}P NMR spectroscopy it is clear that the coupling from phosphorus to the platinum is 366 Hz. The presence of eight phosphines will therefore result in a nonet caused by the ^{31}P nuclei. The observed multiplet is even because of $^1J(Pt-Ag)$, which then must be of the same magnitude as $^2J(Pt-P)$. The Ag isotopes will therefore give rise to two doublets, with a difference of approximately 50 Hz in scalar coupling constants. This results in four overlapping resonances enveloped in the eight most intense lines.

The sharp decrease of $^1J(Pt-Ag)$ when CO is bonded to the parent compound **3** (Table IV) indicates a weakening of the radial bonding in the metal frame; this is also manifest in $^2J(Pt-P)$, which is lowered from 453 to 366 Hz.

Comparison of $\delta(^{195}Pt)$ of the $(S^\sigma)^2(P^\sigma)^4$ and $(S^\sigma)^2(P^\sigma)^6$ clusters presented here shows that the $(S^\sigma)^2(P^\sigma)^4$ clusters resonate at higher frequency than the $(S^\sigma)^2(P^\sigma)^6$ clusters. This difference of approximately 1000 ppm can be attributed to the fact that in the toroidal $(S^\sigma)^2(P^\sigma)^4$ clusters a larger deviation of a spherical valence electron distribution and the low-lying empty P_z^σ result in a larger contribution of the paramagnetic term in the total shielding of the central metal atom. The paramagnetic contribution is known to cause a deshielding of the atom,[18] causing it to resonate at higher frequency.

The IR spectrum shows that $\nu(CO) = 1964\ cm^{-1}$ ($\nu(^{13}CO) = 1918\ cm^{-1}$) is of 24 cm^{-1} higher wavenumber than that of **2**; this suggests that the presence of Ag lowers the π-back-donation, which is consistent with the observed lowering of $^1J(Pt-C)$.

Comparison of the Structures of 3 and 4. Both structures contain a pseudo mirror plane through the atoms Pt, Au1, Au2, and Ag. The distances of some atoms to this plane are given in Table VI. The angles in the plane are as follows: Au1–Pt–Au2 = 147.5 and 169.1°, Au1–Pt–Ag = 150.0 and 124.5°, and Au2–Pt–Ag = 62.4 and 66.4° for **3** and **4**, respectively. The longest Pt–Au bond in **3** is 2.684 Å. This bond is significantly shorter than the shortest one, 2.695 Å, in **4**. Also, the Pt–Ag bond in **3** is shorter than that in **4**. The Pt–Ag distances are in the same range as the Pt–Au distances, which is also found in Pt–Ag and Pt–Au alloys. The Pt–Ag distances are shorter compared to the range 2.77–2.82 Å, which is found in the few other comparable cluster compounds.[6] The Au–Ag distances are in the range as found in other gold–silver clusters.[8] The Au–P distances are in the range normally found for this type of clusters. The mean Au–P bond in **3** is shorter than that in **4**. The platinum–carbon bond distance in **4** is 1.88 Å, which is similar to the 1.896 Å found in $[Pt(CO)(AuPPh_3)_8](NO_3)_2$.[1] The C–O bond length in **4** (1.10 Å) is in the normal range found for metal carbonyls. Comparison of the structures of **3** and **4** shows that the radial bond lengths are longer in **4** than in **3**. This is in agreement with the smaller Pt–P coupling constant in **4** when compared to **3**. Similar differences in $J(Pt-P)$ values of radial bonds are observed when **1** and **2** are compared. This weakening of the radial metal–metal interactions may be attributed to the π-acidity of the incoming ligand. The d–π^*-back-donation from Pt toward CO decreases the overlap of the Pt d orbitals with the σ orbitals of the peripheral groups.

Acknowledgment. This investigation was supported by the Netherlands Foundation for Chemical Research (SON) with fundamental support from the Netherlands Organization for the Advancement of Pure Research (NWO).

Supplementary Material Available: Tables of crystallographic details and additional temperature factors, fractional positional parameters, thermal parameters, and bond distances and angles (21 pages); listings of observed and calculated structure factors (84 pages). Ordering information is given on any current masthead page.

(18) Harris, R. K. *Nuclear Magnetic Resonance Spectroscopy, A Physiochemical View*; Longman Group UK Limited: Harlow, U.K., 1986; §8-6.